

Autonomous system analysis of the late-time cosmological solutions and their stability in $f(Q)$ Gravity Models

Pooja Vishwakarma* and Parth Shah†

Department of Mathematics, School of Advanced Sciences, VIT-AP University, Amaravati 522237, India

Kazuharu Bamba‡

Faculty of Symbiotic Systems Science, Fukushima University, Fukushima 960-1296, Japan

Cosmological dynamics are investigated in detail through systematic procedures by using the autonomous system analyses of gravitational field equations in $f(Q)$ gravity. The explicit analyses of the late-time cosmic evolutions are demonstrated for fundamental three types of models under the presence of non-relativistic matter (i.e., dark matter and baryons) as well as radiation. The stability of cosmological solutions is also explored by examining non-hyperbolic critical points based on the center manifold theory. It is shown that the acceleration of the universe can be achieved with $f(Q)$ gravity. Three different models were considered for the study and dynamical systems analysis technique is incorporated. The main finding of the present analyses is that cosmological solutions in $f(Q)$ gravity can effectively fit observable datasets. This is depicted by phase space portraits and qualitative evolution of the cosmological models.

I. INTRODUCTION

The most significant challenge that theoretical physicist have encountered is the universe's late-time accelerated expansion. Many observational indicators, including type Ia supernovae (SNIa)[1–3], Large Scale Structure (LSS), the Cosmic Microwave Background (CMB), and Baryonic Acoustic Oscillations (BAO) [5–7, 13], have led to the present consensus that the universe is going through an accelerated phase of expansion.

The most extensively accepted theory is that the universe is currently dominated by dark energy. None of the existing dark energy models, however, is entirely acceptable. The cosmological constant model (Λ CDM), with the equation of state $w_\Lambda = -1$, is the most competitive cosmic dark energy model [8–12]. Some popular cosmological data can be accounted for and explained using the cosmological constant, which has proven to be a useful model. Consideration of dynamical dark energy may be required, according to some theoretical reasons. The coincidence problem arises when the dynamics of the universe at later stages are predominantly influenced by the cosmological constant, without a fundamental explanation for this occurrence. Additionally, the fine-tuning problem accentuates the discrepancy between the theoretically predicted value of the cosmological constant and its observed value, posing a significant challenge within cosmology [13]. Both issues remain substantial concerns, lacking comprehensive explanations within current fundamental hypotheses. Many concepts proposing time-varying energy densities for dark energy have emerged in

the literature, aiming to tackle or alleviate the cosmological challenges previously mentioned. These diverse ideas represent attempts to provide alternative explanations or modifications within the framework of dark energy to reconcile observed phenomena with theoretical models [14–19].

Modifying the geometry of spacetime is another technique to explain the universe's current acceleration. To achieve this, we modify the Einstein-Hilbert general relativity (GR) action. Except for non-Lagrangian theories (Modified Newtonian Dynamics-MOND), modified theories of gravity are often represented by the modified Lagrangian density, which is further modified by the inclusion of new geometrodynamical elements to the Einstein-Hilbert action integral [20]. There are numerous such modified theories in existence at present. According to cosmological viability, the $f(R)$, $f(R, T)$, $f(T)$, and the $f(Q)$ gravities are the most successful ones. The arbitrary function of the Ricci scalar curvature R is used to express $f(R)$ gravity. This concept was first introduced by H.A. Buchdahl [21] and further explored in the seminal works of V. Faraoni [22]. This theory is of particular interest since it may give a geometric method for describing inflation [23–25] and solving the dark energy problem [26–30]. In $f(R, T)$ theory [31], the gravitational action is modified by including additional terms involving the Ricci scalar (R) and the energy-momentum tensor (T) that describes the distribution of matter and energy in spacetime.

An alternative method to describe gravitational interactions involves torsion and non-metricity. Gravities derived from these characteristics are referred to as GR analogues. Modified versions of these gravities are known as $f(T)$ and $f(Q)$ gravities [32–35]. These gravitational theories can be realized by utilizing non-standard metric-affine connections, such as the Weitzenböck connection and metric incompatible connections, distinct from the Levi-Civita connection in General Rel-

* poojavishwakarma041993@gmail.com; Department of Mathematics, School of Advanced Sciences, VIT-AP University, Amaravati 522237, India

† parthshah2908@gmail.com

‡ bamba@sss.fukushima-u.ac.jp

ativity (GR). These frameworks explore gravitational dynamics beyond the conventional GR paradigm by incorporating different geometric structures and connections. Absolutely, in the realm of General Relativity (GR), the Levi-Civita connection is linked to curvature while maintaining zero torsion. Contrastingly, in the teleparallelism framework, the Weitzenböck connection is tied to torsion while possessing zero curvature. This distinction between the two connections encapsulates their primary geometric characteristics and illustrates their role in describing gravitational interactions within their respective gravitational theories [36]. The $f(T)$ gravity is also the most easily understood teleparallel equivalent of general relativity (TEGR) [37–39]. A new type of gravity theory, the symmetric teleparallel equivalent of general relativity (STEGR), has recently been investigated. The concept of non-metricity scalar Q is used in this theory to define gravitational interactions which has zero torsion and curvature [40, 41] (for recent review on $f(Q)$ gravity, see [42]). The STEGR’s most straightforward modification is $f(Q)$ gravity. Both teleparallel and symmetric teleparallel gravity can be built on fascinating geometric frameworks provided by torsion and non-metricity, respectively [43–51]. In this study, we consider the case of modified symmetric teleparallel gravity.

One of the primary concerns with theories of gravity is that their non-linear components in the field equations make it difficult to obtain analytical or numerical solutions, which makes it difficult to compare them with observations. Such equations can be solved or the general behaviour can be studied or analyzed using the “Dynamical System Analysis” technique. In order to describe the qualitative behaviour of a certain physical system, this technique looks for the numerical solutions [52–54]. Dynamical system analysis focuses on identifying critical points within a set of first-order ordinary differential equations [55, 56]. Determining the stability involves computing the Jacobian matrix at these critical points and evaluating its eigenvalues. Linearizing the system around each critical point helps discern the system’s behavior and stability properties in the vicinity of that point. This approach allows for an in-depth investigation into the flow and stability characteristics around specific critical points within the system [57–64]. For non-hyperbolic points, linear stability fails. A critical point, known as a non-hyperbolic point, if it has zero real part among its eigenvalues (a critical point is considered hyperbolic if none of its eigenvalues is zero)[63]. It’s worth noting that the paper [63] discusses perturbation, while the current work does not. In these cases, the stability properties of the system must be studied using other techniques, such as Center Manifold Theory and Lyapunov Functions. In this work, we are using “Center Manifold Theory” to study the stability properties of non-hyperbolic points.

In this work, driven by the fascinating features of $f(Q)$ gravity, we investigate the cosmic dynamics of the $f(Q)$ gravity models at background levels utilising the mathe-

tical tool of dynamical system analysis. These studies can be utilised to support the findings of the observational analysis. The paper is organised as follows. In Sec. II, we presents the $f(Q)$ gravity field equations, from which the background cosmological equations can be obtained. In sec. III, we describe the formalism of the Center Manifold Theory. In Sec. IV, we investigate the dynamical analysis of the coupled system for the power-law model, exponential model and logarithmic model. Finally, the results are summarised in Sec. V.

II. $f(Q)$ COSMOLOGY

Indeed, Lorentzian Geometry forms the basis of General Relativity by adopting a symmetric and metric-compatible connection. The Levi-Civita connection, utilized in General Relativity, embodies these traits. Its defining characteristic lies in generating non-zero curvature while maintaining zero torsion and non-metricity. This specific connection captures the geometric framework crucial for describing gravitational phenomena within the context of General Relativity [65]. However, in the framework of geometrodynamics as the foundational theory for gravity, a broader range of connections becomes accessible. The most general form of connection in this context is termed the metric-affine connection, and it is expressed by the formula

$$\Gamma_{\mu\nu}^{\beta} = \{\beta_{\mu\nu}\} + K_{\mu\nu}^{\beta} + L_{\mu\nu}^{\beta} ,$$

where the Christoffel symbols of the Levi-Civita connection $\{\beta_{\mu\nu}\}$ is defined by

$$\{\beta_{\mu\nu}\} = \frac{1}{2}g^{\beta\sigma}(\partial_{\mu}g_{\sigma\nu} + \partial_{\nu}g_{\sigma\mu} - \partial_{\sigma}g_{\mu\nu}) ,$$

$L_{\mu\nu}^{\beta}$ is the deformation represented by

$$L_{\mu\nu}^{\beta} = \frac{1}{2}Q_{\mu\nu}^{\beta} - Q_{(\mu\nu)}^{\beta} ,$$

and the contorsion $K_{\mu\nu}^{\beta}$ is given by

$$K_{\mu\nu}^{\beta} = \frac{1}{2}T_{\mu\nu}^{\beta} + T_{(\mu\nu)}^{\beta} ,$$

with the anti-symmetric part of the affine connection, the torsion tensor $T_{\mu\nu}^{\beta}$ is defined as

$$T_{\mu\nu}^{\beta} = 2\Gamma_{[\mu\nu]}^{\beta} .$$

Thus, the three geometric deformations $\{\beta_{\mu\nu}\}$, $L_{\mu\nu}^{\beta}$ and $K_{\mu\nu}^{\beta}$ provide a sort of “trinity of gravity” that includes all elements of the general connection $\Gamma_{\mu\nu}^{\beta}$ [65]. This effectively indicates that the geometry of a gravitational theory can be expressed in torsion, non-metricity, or curvature. Acceptance of non-metricity in affine connection with zero curvature and torsion is referred to as Symmetric Teleparallel Gravity connection, whereas connections which have only zero curvature are referred to as Teleparallel connections. The non-metricity tensor is given by

$$Q_{\lambda\mu\nu} = \nabla_\lambda g_{\mu\nu} = \partial_\lambda g_{\mu\nu} - \Gamma_{\lambda\mu}^\beta g_{\beta\nu} - \Gamma_{\lambda\nu}^\beta g_{\mu\beta}.$$

The symmetric teleparallel gravity, often referred to as $f(Q)$ gravity, was initially formulated by Jimenez and colleagues [40, 41]. This gravitational theory explores a symmetric teleparallel framework that utilizes the quantity Q , offering an alternative approach to understanding gravitational interactions beyond the traditional descriptions found in General Relativity. The action of modified gravity is given by

$$S = \int \left[-\frac{1}{16\pi G} f(Q) + \mathcal{L}_m \right] \sqrt{-g} d^4x, \quad (1)$$

where the Lagrangian density of matter is \mathcal{L}_m , and g is the determinant of the metric tensor $g_{\mu\nu}$. An arbitrary function of Q , the non-metricity scalar that drives the gravitational interaction, is $f(Q)$. The corresponding field equation is given by

$$\begin{aligned} \sqrt{-g} \left(\frac{1}{2} f_{g_{\mu\nu}} - \frac{\partial f}{\partial g^{\mu\nu}} \right) - 2\nabla_\alpha (\sqrt{-g} P_{\mu\nu}^\alpha) \\ = 8\pi G \sqrt{-g} T_{\mu\nu} \end{aligned} \quad (2)$$

with

$$\frac{\partial f}{\partial g^{\mu\nu}} = -\frac{f_Q}{\sqrt{-g}} \left(\frac{\partial(\sqrt{-g}Q)}{\partial g^{\mu\nu}} - \frac{1}{2} \sqrt{-g} Q g_{\mu\nu} \right), \quad (3)$$

the conjugate to $f(Q)$ is defined as [75]

$$P_{\mu\nu}^\alpha = \frac{1}{2\sqrt{-g}} \frac{\partial(\sqrt{-g}f(Q))}{\partial Q_{\mu\nu}^\alpha}, \quad (4)$$

$T_{\mu\nu}$ is the matter energy-momentum tensor, whose form is

$$T_{\mu\nu} = -\frac{2}{\sqrt{-g}} \frac{\delta(\sqrt{-g}\mathcal{L}_m)}{\delta g^{\mu\nu}}, \quad (5)$$

and $f_Q = \frac{\partial f}{\partial Q}$. The non-metricity scalar Q is represented as

$$Q = -\frac{1}{4} Q_{\alpha\beta\gamma} Q^{\alpha\beta\gamma} + \frac{1}{2} Q_{\alpha\beta\gamma} Q^{\gamma\beta\alpha} + \frac{1}{4} Q_\alpha Q^\alpha - \frac{1}{2} Q_\alpha \bar{Q}^\alpha, \quad (6)$$

where

$$Q_\alpha \equiv Q_{\alpha\mu}{}^\mu \text{ and } \bar{Q}^\alpha \equiv Q_\mu{}^{\mu\alpha}$$

comprises of two independence traces. By condensing the non-metricity tensor

$$Q_{\alpha\mu\nu} \equiv \nabla_\alpha g_{\mu\nu},$$

we obtained the above independence traces, which help us to define the non-metricity scalar as $Q = -Q_{\alpha\mu\nu} P^{\alpha\mu\nu}$, where $P^{\alpha\mu\nu}$ is the non-metricity conjugate because it satisfies

$$P^{\alpha\mu\nu} = -\frac{1}{2} \frac{\partial Q}{\partial Q_{\alpha\mu\nu}}$$

With regard to changes over the metric tensor, the metric field equations can be written as

$$\begin{aligned} \frac{2}{\sqrt{-g}} \nabla_\alpha \sqrt{-g} g_{\beta\nu} f_Q \left[-\frac{1}{2} L^{\alpha\mu\beta} + \frac{1}{4} g^{\mu\beta} (Q^\alpha - \bar{Q}^\alpha) \right. \\ \left. - \frac{1}{8} (g^{\alpha\mu} Q^\beta + g^{\alpha\beta} Q^\mu) \right] + f_Q \left[-\frac{1}{2} L^{\mu\alpha\beta} - \frac{1}{8} (g^{\mu\alpha} Q^\beta + \right. \\ \left. g^{\mu\beta} Q^\alpha) + \frac{1}{4} g^{\alpha\beta} (Q^\alpha - \bar{Q}^\alpha) \right] Q_{\nu\alpha\beta} + \frac{1}{2} \delta_\nu^\mu = 8\pi G \sqrt{-g} T_\nu^\mu, \end{aligned} \quad (7)$$

In the background level, we assume a homogeneous, isotropic, spatially flat Friedmann-Lemaitre-Robertson-Walker (FLRW) spacetime with a metric of the form

$$ds^2 = -N^2(t) dt^2 + a^2(t) (dx^2 + dy^2 + dz^2), \quad (8)$$

where $N(t)$ is a Lapse function and t is the cosmic time. We shall now fix the coincident gauge so the connection is trivial, unless otherwise indicated. Then, $Q = \frac{6H^2}{N^2}$ is the non-metricity scalar. One would assume that we are not permitted to choose any specific lapse function because we fixed the coincident gauge using diffeomorphisms. But since Q retains a residual time-reparameterization invariance [67, 68], the particular case of $f(Q)$ theories prevents this, thus we will leverage this symmetry to set $N = 1$. The Hubble function, $H = \frac{\dot{a}}{a}$, indicates the rate of expansion of the universe at time t . The notation ‘.’ indicates a derivative with regard to t [63]. The cartesian coordinates are x, y, z , and the function $a(t)$, also referred to as the scale factor, represents the size of the universe at time t . To derive the field equations, for simplicity we set $8\pi G = 1$, and imposing the splitting $f(Q) = Q + F(Q)$ and using the FLRW metric [40, 41, 66, 69–73]. The corresponding field equations are

$$3H^2 = (\rho_m + \rho_r) + \frac{F}{2} - QF_Q, \quad (9)$$

$$(2QF_{QQ} + F_Q + 1)\dot{H} + \frac{1}{4}(Q + 2QF_Q - F) = -2(P_m + P_r), \quad (10)$$

where $F_Q = \frac{dF}{dQ}$, $F_{QQ} = \frac{d^2F}{dQ^2}$, ρ_m , ρ_r and P_m , P_r are the energy densities and pressures of the matter and radiation perfect fluids respectively. They fulfill the fluid equation or the energy conservation equation in the absence of interaction, which is provided by

$$\dot{\rho}_m + 3H(\rho_m + P_m) = 0 \quad (11)$$

$$\dot{\rho}_r + 3H(\rho_r + P_r) = 0 \quad (12)$$

with $P = \rho w$ serving as the linear equation of state parameter w between them, where $w \in [-1, 1]$, the equation of state parameter.

However, ‘‘matter’’ refers to the mixture of dark matter and baryonic matter. Together, these two types of matter

account for the bulk of the universe's mass, with dark matter dominating in terms of mass while being unseen and undetectable by traditional techniques. On the other hand, we can directly observe and interact with baryonic matter.

From the Friedmann's equation (11), we have

$$1 = \frac{\rho_m + \rho_r}{3H^2} + \frac{\frac{F}{2} - QF_Q}{3H^2}.$$

One needs $w_{\text{eff}} < -\frac{1}{3}$ for an accelerating universe [58, 60, 75]. Thus, it is convenient to define Ω_m and Ω_Q , the energy density parameters, as

$$\begin{cases} \Omega_m = \frac{\rho_m}{3H^2} \\ \Omega_Q = \frac{\frac{F}{2} - QF_Q}{3H^2} \\ \Omega_r = \frac{\rho_r}{3H^2} \end{cases} \quad (13)$$

Hence, the Friedmann's equation (9) can be simply written as

$$\Omega_m + \Omega_Q + \Omega_r = 1. \quad (14)$$

The effective total energy density ρ_{eff} and total energy pressure P_{eff} , is represented as [66]

$$\rho_{\text{eff}} \equiv \rho_m + \rho_r + \frac{F}{2} - QF_Q, \quad (15)$$

$$P_{\text{eff}} \equiv \frac{(\rho_m + P_m + \rho_r + P_r)}{2QF_{QQ} + F_Q + 1} - \frac{Q}{2}. \quad (16)$$

The corresponding total equation of state (EoS) w_{eff} can be written as

$$w_{\text{eff}} = \frac{P_{\text{eff}}}{\rho_{\text{eff}}}. \quad (17)$$

III. CENTER MANIFOLD THEORY

Three theorems will be used to investigate the stability of orbits in the center manifold. The first demonstrates the center manifold's existence, and the second one deals with stability. The last theorem demonstrates how to build the real center manifold locally and that doing so is sufficient to look into the stability [74, 75]. Consider the dynamical system

$$\xi' = F(\xi)$$

where, $\xi = (\mu, \nu)$ which can be rewritten in the form

$$\mu' = A\mu + \varphi(\mu, \nu), \quad \nu' = B\nu + \psi(\mu, \nu) \quad (18)$$

where $(\mu, \nu) \in \mathbb{R}^\alpha \times \mathbb{R}^\beta$ with α and β , the dimension of \mathbb{E}^α and \mathbb{E}^β respectively, and the functions φ and ψ satisfies

$$\varphi(0, 0) = 0, \quad \nabla\varphi(0, 0) = 0,$$

$$\psi(0, 0) = 0, \quad \nabla\psi(0, 0) = 0,$$

where ∇ is the gradient, and \mathbb{E}^α and \mathbb{E}^β are the center and stable subspaces, respectively, spanned by the eigenvectors of the Jacobian matrix associated with eigenvalues with zero real part and negative real part, respectively. Also, In system (18), A and B are square matrices of order $\alpha \times \alpha$ and $\beta \times \beta$ having eigenvalues with zero real part and negative real part respectively. A geometrical space is a centre manifold for (18) if it can be locally represented as

$$W^\alpha(0) = \{(\mu, \nu) \in \mathbb{R}^\alpha \times \mathbb{R}^\beta : \nu = h(\mu), \quad |\mu| < \delta, \quad h(0) = 0, \quad \nabla h(0) = 0\}$$

for δ sufficiently small and $h(\mu)$ is (sufficiently regular) function on \mathbb{R}^β

Definition 1 (Stable Fixed Point)

A fixed point ξ_0 of the system $\xi' = F(\xi)$ is stable if for every $\varepsilon > 0$, we can find a δ such that for any solution $\eta(t)$ of system $\xi' = F(\xi)$ satisfying $\|\eta(t_0) - \xi_0\| < \delta$, then the solution $\eta(t)$ exists for all $t \geq t_0$ and it will satisfy $\|\eta(t) - \xi_0\| < \varepsilon$ for all $t \geq t_0$.

In simple words, a fixed point ξ_0 within a system described by $\xi' = F(\xi)$ is deemed stable if all solutions $\xi(t)$, which begin close to ξ_0 , stay in the vicinity of this point as time progresses. In essence, it means that nearby points gravitate towards and remain near ξ_0 over time.

Definition 2 (Asymptotically Stable Fixed Point)

A fixed point ξ_0 of the system $\xi' = F(\xi)$ is called asymptotically stable if for every $\varepsilon > 0$, we can find a δ such that for any solution $\eta(t)$ of system $\xi' = F(\xi)$ satisfying $\|\eta(t_0) - \xi_0\| < \delta$, then $\lim_{\mu \rightarrow \infty} \eta(t) = \xi_0$.

In another way, a fixed point ξ_0 in the system $\xi' = F(\xi)$ is considered asymptotically stable if it meets two criteria:

1. Stability: Solutions starting close to ξ_0 remain in proximity to it.

2. Attractiveness: Solutions from nearby initial conditions gravitate toward ξ_0 as time progresses, indicating that the critical point is a point of attraction for the system.

Physically, if a system is both stable and its perturbations from its equilibrium state gradually approach zero over time, it is referred to as "asymptotically stable." It indicates that after being perturbed, the system not only returns to its equilibrium state but also converges towards it, with the deviations decreasing as time approaches infinity.

Theorem 1 (Existence)

There exists a centre manifold for equation (18). The dynamics of the system (18) restricted to the centre manifold is given by

$$v' = Av + \varphi(v, h(v)) \quad (19)$$

for $v \in \mathbb{R}^\alpha$ is sufficiently small.

Theorem 2 (Stability)

Assume that (18) has a stable zero solution (either asymptotically stable or unstable). Then the zero solution of (19) is also stable (asymptotically stable or unstable). Furthermore, if $(\mu(t), \nu(t))$ is also a solution of (18) with $(\mu(0), \nu(0))$ sufficiently small, there exists a solution $v(t)$ of (19) such that

$$\begin{aligned}\mu(t) &= v(t) + \mathcal{O}(e^{-\delta t}) \\ \nu(t) &= h(v(t) + \mathcal{O}(e^{-\delta t}))\end{aligned}$$

as $t \rightarrow \infty$, where $\delta > 0$ is a constant.

Theorem 3 (Approximation)

Let $\Psi : \mathbb{R}^\alpha \rightarrow \mathbb{R}^\beta$ be a mapping with $\Psi(0) = \nabla\Psi(0) = 0$ such that $\mathcal{N}(\Psi(\mu)) = \mathcal{O}(|\mu|^q)$ as $\mu \rightarrow 0$ for some $q > 0$. Then

$$|h(\mu) - \Psi(\mu)| = \mathcal{O}(|\mu|^q) \text{ as } \mu \rightarrow 0$$

IV. DYNAMICAL SYSTEM ANALYSIS

The dynamical system is constructed in this section for a generic function $F(Q)$.

Case 1. Only matter

The following dynamical variables are taken into consideration as we convert the equations (11)–(14) into a first order autonomous system [63]:

$$p = \frac{F}{6H^2}, \quad q = -2F_Q. \quad (20)$$

The background evolution of the universe is connected to the variables p and q . Ω_m , Ω_Q , and w_{eff} are cosmic background parameters. These can be represented as [40]

$$\begin{aligned}\Omega_m &= 1 - p - q, \\ \Omega_Q &= p + q, \\ w_{\text{eff}} &= -1 + \frac{(1-p-q)(1+\omega_m)}{2QF_{QQ} - \frac{q}{2} + 1}.\end{aligned} \quad (21)$$

Now, using the variables from equation (20), the cosmological equations can be written as the following dynamical system:

$$p' = -\frac{\dot{H}}{H^2}(q+2p), \quad (22)$$

$$q' = -\frac{\dot{H}}{H^2}4QF_{QQ}, \quad (23)$$

where $(\dot{})$ indicates differentiation with respect to t and (\prime) indicates differentiation with respect to $\ln a$ and

$$\frac{\dot{H}}{H^2} = \frac{3(p+q-1)}{4QF_{QQ} - q + 2}. \quad (24)$$

Case 2. Matter combined with radiation

Accordingly, we consider the following dynamical variables in order to transform the equations (11)–(14) into first order autonomous systems:

$$p = \frac{F}{6H^2}, \quad q = -2F_Q, \quad r = \frac{\rho_r}{3H^2}. \quad (25)$$

Variables p , q and r are related to universe's background evolution. Ω_m , Ω_Q , Ω_r , and w_{eff} are cosmic background parameters. These can be represented as [40]

$$\Omega_m = 1 - p - q - r,$$

$$\Omega_Q = p + q,$$

$$\Omega_r = r,$$

$$w_{\text{eff}} = -1 + \left(\frac{\Omega_m + \frac{4}{3}r}{2QF_{QQ} + F_Q + 1} \right). \quad (26)$$

Using the variables from equation (25), the cosmological equations can be written as the following dynamical system:

$$p' = -\frac{\dot{H}}{H^2}(q+2p), \quad (27)$$

$$q' = -\frac{\dot{H}}{H^2}4QF_{QQ}, \quad (28)$$

$$r' = -2r(2 + \frac{\dot{H}}{H^2}), \quad (29)$$

and we have

$$\frac{\dot{H}}{H^2} = \frac{-4r + 3(p+q-1)}{4QF_{QQ} - q + 2}. \quad (30)$$

In the next stage, we explore the system's critical points and assess their stability in order to explain the dynamical evolution of the system. Before beginning the specific analysis and establishing the term QF_{QQ} , we must first define the function F . In the subsections that follow, we specifically address three models namely the power-law model, the exponential model and the logarithmic model known to offer a fascinating cosmic phenomenology.

A. MODEL I : $f(Q) = Q + \kappa(\frac{Q}{Q_0})^n$

Considering the power-law model

$$f(Q) = Q + \kappa\left(\frac{Q}{Q_0}\right)^n \quad (31)$$

with having two parameters, κ and n while $Q_0 = 6H_0^2$ is the present value of Q (it is observed that κ can be

removed in terms of n and the current value Ω_{m0} by using the first Friedmann equation at the present time). In accordance with the Big Bang Nucleosynthesis (BBN) criterion, this model explains the acceleration of cosmos in the late universe [73, 76–79]. It is seen that this model simplifies to the symmetric teleparallel theory of general relativity for $n = 0$ and $n = 1$, the concordance Λ CDM scenario [61, 80]. We also find

$$QF_{QQ} = \frac{(1-n)}{2}q.$$

Power-law models allow systematic analysis of how power-law exponent values affect theory behaviour, making them theoretically intriguing. Such models can be compared to more complex functional forms for faster analytical solutions and stability checks. By choosing appropriate power-law exponent values, these models can mimic cosmic expansion history, including accelerated expansion, without anomalous dark energy components. Study-based validation CMB studies, large-scale structure surveys, and supernova data can validate power-law models. This allows researchers to constrain model parameters and assess model agreement with experimental results. Power-law models can reveal screening mechanisms, where gravity adjustments only matter on cosmological scales. The hypothesis can be consistent with smaller-scale gravity studies like solar system experiments while allowing for larger-scale aberrations using these methods. The power-law exponent can be modified to study various gravitational behaviours in $f(Q)$ gravity. This parameter space inquiry is essential to understand and compare prospective predictions to observations.

In conclusion, power-law models in $f(Q)$ gravity help test different gravity theories. They allow us to test General Relativity, investigate cosmic acceleration, and study gravity at different sizes. These models help us understand the universe's expansion and gravitational physics.

Case 1. Only matter

The system (22)–(24) becomes

$$p' = \frac{3(1-p-q)}{q(1-2n)+2}(q+2p), \quad (32)$$

$$q' = \frac{3(1-p-q)}{q(1-2n)+2}2(1-n)q, \quad (33)$$

Corresponding to this dynamical system, there are two critical points:

* **Critical Point** $(p, 1-p)$: This point's curve corresponds to a solution with the energy density $\Omega_m = 0$, which means that there is no matter contribution to the total energy density of the universe in the context of symmetric teleparallel gravity. On the other hand, the energy density $\Omega_Q = 1$, which means that dark energy completely dominates the total energy density of the universe. A cosmological constant-like acceleration of the

universe is $w_{\text{eff}} = -1$. The observed accelerated expansion of the universe is driven exclusively by the repulsive effects of dark energy, with no significant input from matter. With one vanishing eigenvalue along with an other eigenvalue -3 , the curve is one-dimensional. Looking at the non-vanishing eigenvalue, the curve is stable. The critical point $(p, 1-p)$ exhibits non-hyperbolic behavior due to the presence of one eigenvalue that equals zero within the associated Jacobian matrix. Utilizing center manifold theory, we establish the system's asymptotic stability at this equilibrium point.

The central variable in this instance is p , while the stable variable is q . The matrices that correlate are $B = -3$ and $A = 0$. The center manifold has now the form $q = h(p)$; the approximation \mathcal{N} is given by

$$\mathcal{N}(h(p)) = h'(p) \frac{3(1-p-h(p))}{h(p)(1-2n)+2}(h(p)+2p) - \frac{3(1-p-h(p))}{h(p)(1-2n)+2}2(1-n)h(p)$$

For zeroth approximation:

$$\mathcal{N}(h(p)) = 0 + \mathcal{O}(p^2)$$

Therefore the reduced equation is written as

$$p' = -3p + \mathcal{O}(p^2)$$

This has negative linear term. Therefore, the system of equation (32)–(33) is asymptotically stable as per the central manifold theory.

In essence, the discussion highlights the significance of the curve $(p, 1-p)$, showcasing the late time dark-energy dominated universe.

* **Critical Point** $(0, 0)$: The matter dominance at the background level is indicated at this position, where $w_{\text{eff}} = 0$ and $\Omega_m = 1$. Since the eigenvalues of the Jacobian matrix are $(3, -3(n-1))$, this point is saddle for $n > 1$ and unstable for $n \leq 1$. This point represents the era where matter formation is completed and the point may be saddle or unstable depending on the value of n . Energy density $\Omega_m = 1$, it means that the matter component completely dominates the total energy density of the universe in the context of symmetric teleparallel gravity. This implies that matter, including both ordinary matter (baryonic matter) and dark matter, accounts for the entirety of the energy density.

Case 2. Matter combined with radiation

Hence the system (27)–(30) becomes

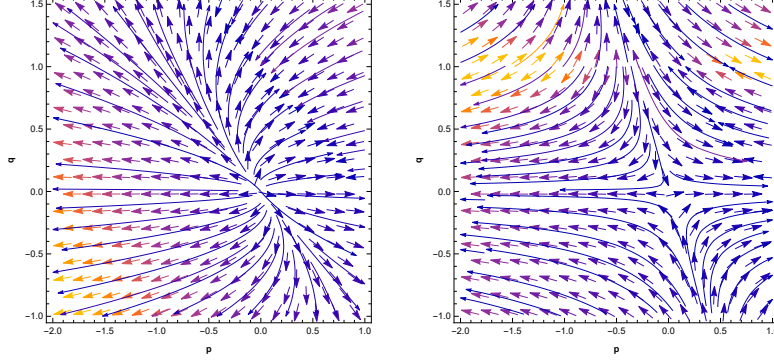
$$p' = \frac{4r+3(1-p-q)}{q(1-2n)+2}(q+2p), \quad (34)$$

$$q' = \frac{4r+3(1-p-q)}{q(1-2n)+2}2(1-n)q, \quad (35)$$

$$r' = -2r \left(2 + \frac{-4r+3(p+q-1)}{q(1-2n)+2} \right). \quad (36)$$

TABLE I. Critical points, stability conditions and the EoS parameter.

Critical Points	Eigen-Values	Ω_m	Ω_Q	w_{eff}	Stability Condition
$(p, 1-p)$	$(0, -3)$	0	1	-1	Stable
$(0, 0)$	$(3, -3(n-1))$	1	0	0	Saddle for $n > 1$ and Unstable for $n \leq 1$

FIG. 1. Phase portrait for the dynamical system of Model I, (i) for $n = 0.5$; (ii) for $n = \frac{3}{2}$.

Corresponding to this dynamical system, there are three critical points:

* **Critical Point** $(p, 1-p, 0)$: At this point, the curve implies a solution where $w_{\text{eff}} = -1$, the universe accelerates, and the effective dark energy component dominates, or $\Omega_Q = 1$. This solution reflects the behavior of a cosmological constant. The curve has one vanishing eigenvalue and two additional eigenvalues, -4 and -3 . It is one-dimensional. The stability of the curve can be evaluated by examining the signature of non-zero eigenvalues. The point's curve is therefore continuously stable. Furthermore, since the related Jacobian matrix has a single vanishing eigenvalue, the critical point $(p, 1-p, 0)$ is non-hyperbolic. We find that the system of equations is asymptotically stable by applying the center manifold theory method.

In this instance, the stable variables are q, r , while the central variable is p . The corresponding matrices are $A = 0$ and $B = \begin{pmatrix} -4 & 0 \\ 0 & -3 \end{pmatrix}$. The center manifold has now the form $q = h_1(p)$ and $r = h_2(p)$. The two components of the approximation \mathcal{N} are:

$$\mathcal{N}_1(h_1(p)) = h_1'(p) \frac{4h_2(p) + 3(1-p-h_1(p))}{h_1(p)(1-2n)+2} (h_1(p) + 2p) - \frac{4h_2(p) + 3(1-p-h_1(p))}{h_1(p)(1-2n)+2} 2(1-n)h_1(p),$$

$$\mathcal{N}_2(h_2(p)) = h_2'(p) \frac{4h_2(p) + 3(1-p-h_1(p))}{h_1(p)(1-2n)+2} (h_1(p) + 2p) + 2h_2(p) \left(2 + \frac{-4h_2(p) + 3(p+h_1(p)-1)}{h_1(p)(1-2n)+2} \right)$$

For zeroth approximation:

$$\mathcal{N}_1(h_1(p)) = 0 + \mathcal{O}(p^2)$$

and

$$\mathcal{N}_2(h_2(p)) = -\frac{7}{2} + 3p + \mathcal{O}(p^2)$$

Therefore the reduced equation gives us

$$x' = -11p + \mathcal{O}(p^2)$$

This provides the negative linear portion. Thus, according to the central manifold theory, the system of equations (34)–(36) is stable at the equilibrium point. Hence, the discussion emphasizes the importance of the curve $(p, 1-p, 0)$, which illustrates the late-time dark-energy dominated cosmos.

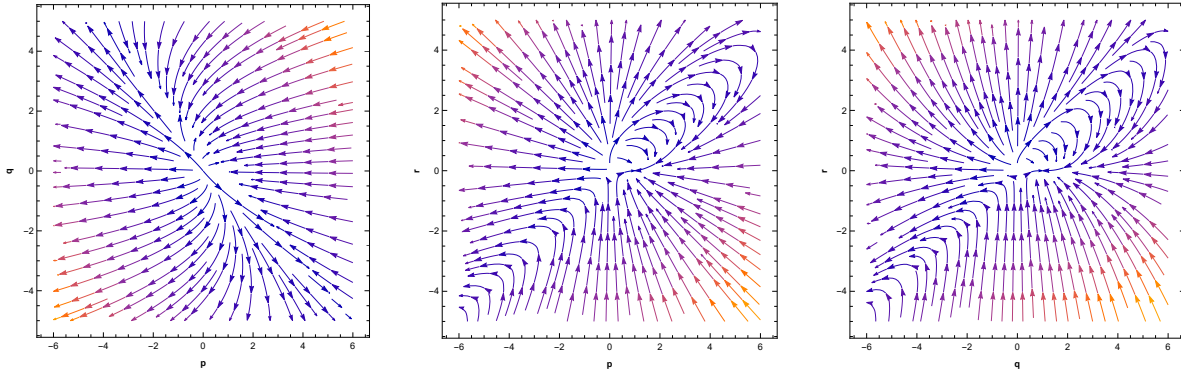
* **Critical Point** $(0, 0, 0)$: The critical point $(0, 0, 0)$ signifies a scenario where $\Omega_m = 1$, $\Omega_Q = 0$, $\Omega_r = 0$, and $w_{\text{eff}} = 0$, emphasizing the supremacy of matter at the background level. Despite having eigenvalues $(3, -1, -3(n-1))$ for all n , this point serves as a saddle. Trajectories pass through this point, subsequently diverging as they approach a late-time stable point. This observation leads us to consider this scenario as a compelling explanation for the formation of structures during the matter-dominated period at background levels.

* **Critical Point** $(0, 0, \frac{1}{4})$: This particular point is characterized by $\Omega_m = \frac{3}{4}$, $\Omega_Q = 0$, $\Omega_r = \frac{1}{4}$, and $w_{\text{eff}} = \frac{1}{12}$. It signifies an epoch where matter, radiation, and dark energy coexist. The eigenvalues of the Jacobian matrix at this critical point are $(4, 1, -4(n-1))$. For $n \leq 1$, this point proves to be unstable, while for $n > 1$, it exhibits saddle-like behavior.

In Fig. 3, the initial phase shows the universe predominantly filled with radiation, gradually diminishing as matter formation progresses, leading to an increase in its relative energy density. Eventually, in the latter

TABLE II. Critical points, stability conditions and the EoS parameter.

Critical Points	Eigen-Values	Ω_m	Ω_Q	$\Omega_r = r$	w_{eff}	Stability Condition
$(p, 1-p, 0)$	$(0, -4, -3)$	0	1	0	-1	Stable
$(0, 0, 0)$	$(3, -1, -3(n-1))$	1	0	0	0	Saddle
$(0, 0, \frac{1}{4})$	$(4, 1, -4(n-1))$	$\frac{3}{4}$	0	$\frac{1}{4}$	$\frac{1}{12}$	Unstable for $n \leq 1$, Saddle for $n > 1$

FIG. 2. Phase portrait for the dynamical system of Model I, (i)left panel($r = 0$ and $n = 0.5$); (ii)middle panel($q = 0$); (iii)right panel($p = 0$ and $n = 0.5$).

stages, the dominance of dark energy initiates and drives the observed acceleration in the universe's expansion.

The parameter w_{eff} reflecting the equation of state starts at $\frac{1}{3}$ when radiation dominates the universe entirely. It decreases to zero during the epoch of matter formation, eventually turning negative and reaching its ultimate value of $w_{\text{eff}} = -1$ as dark energy gradually ascends to dominance. This evolution of w_{eff} delineates the transitions between radiation, matter, and dark energy eras within the cosmic history showcased in Fig. 3.

B. MODEL II : $f(Q) = Qe^{\kappa(\frac{Q_0}{Q})}$

In this subsection we consider the exponential model

$$f(Q) = Qe^{\kappa(\frac{Q_0}{Q})}, \quad (37)$$

with having the only one dimensionless parameter κ . For $\kappa = 0$ the model is equivalent to GR without a cosmological constant. The model can fit observations extremely satisfactorily for $\kappa \neq 0$, despite the fact that it does not contain a cosmological constant. Note that κ can be eliminated in terms of Ω_{m0} by using the first Friedmann equation at present. Additionally, because the model tends to GR limit at early times when $Q \gg Q_0$, it easily satisfies the BBN constraints [73, 76–79]. As

$$QF_{QQ} = \frac{(p+1)^2 + p(q-2) + \frac{q^2}{4} - 1}{p+1},$$

Exponential functions are easy to calculate. They can be used to study $f(Q)$ gravity fundamentals and find easy analytical solutions. The exponential function can explain observable evidence on the cosmic microwave back-

ground (CMB) and supernovae associated to the universe's accelerated expansion, depending on its shape. Some exponential $f(Q)$ gravity models match observable evidence. These models can provide GR alternatives that match cosmological and astrophysical observations. By modifying exponential model parameters, researchers can study gravitational dynamics and deviations from general relativity.

In conclusion, exponential models in $f(Q)$ gravity help test various gravity theories. They provide a framework to study dark energy, General Relativity, gravity on multiple scales, and dark energy-dark matter correlations. These models aid our understanding of the universe's core forces.

Case 1. Only matter

The system (22)–(24) becomes

$$p' = \frac{3(1-p-q)}{\frac{(2p+q)^2}{p+1} - q + 2}(q+2p), \quad (38)$$

$$q' = \frac{3(1-p-q)}{(2p+q)^2 - (q-2)(p+1)}(2p+q)^2 \quad (39)$$

In this case, the system has two curves of critical points

* **Critical Point $(p, 1-p)$:** The curve at this point is consistent with a solution where the energy density $\Omega_m = 0$, indicating that matter does not contribute to the overall energy density of the universe. However, the energy density $\Omega_Q = 1$ indicates that dark energy dominates the universe's overall energy density. This would

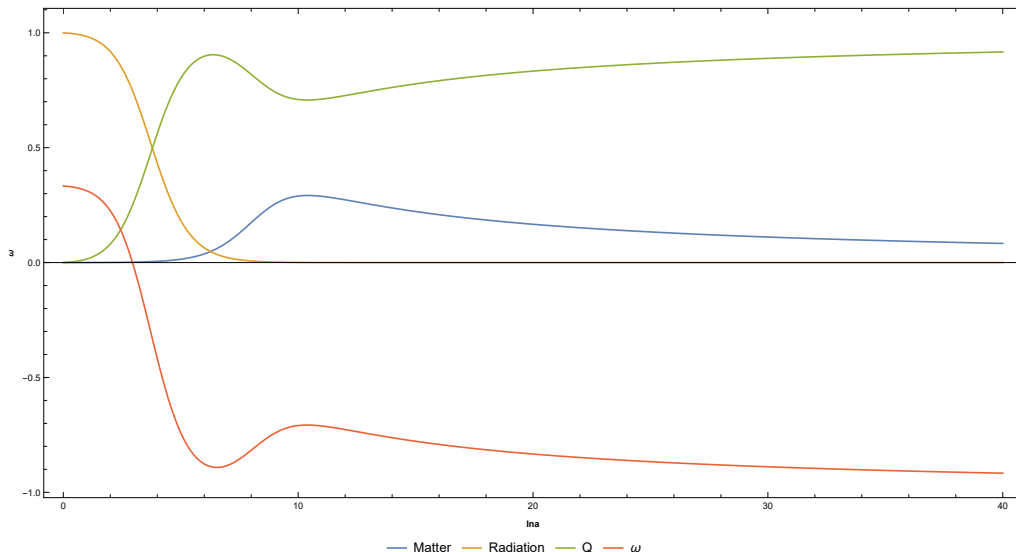


FIG. 3. Evolution of matter, radiation, Q =Dark energy and the EoS parameter in the power-law model.

TABLE III. Critical points, stability conditions and the EoS parameter.

Critical Points	Eigen-Values	Ω_m	Ω_Q	w_{eff}	Stability Condition
$(p, 1 - p)$	$(-3, 0)$	0	1	-1	Stable
$(p, -2p)$	$(3, 0)$	$1 + p$	$-p$	0	Unstable

suggest that the universe's apparent accelerated expansion is purely caused by the repelling effects of dark energy, without any major contribution from matter. Indeed, in line with the anticipated behavior resembling that of a cosmological constant, the universe experiences acceleration characterized by $w_{\text{eff}} = -1$.

The curve under examination is one-dimensional, featuring eigenvalues of 0 and -3 . Analyzing the non-vanishing eigenvalue, we determine the curve's stability. Additionally, due to the non-hyperbolic nature of the critical point $(p, 1 - p)$, the application of center manifold theory confirms the system's asymptotic stability.

In this case q and h are the central and stable variables respectively. The corresponding matrices are $A = -3$ and $B = 0$. Now, the center manifold has the form $p = h(q)$; the approximation \mathcal{N} is given by

$$\mathcal{N}(h(q)) = h'(q) \frac{3(1-h(q)-q)}{u(q)-q+2} u(q) - \frac{3(1-h(q)-q)}{u(q)-q+2} (q + 2h(q))$$

$$\text{where } u(q) = \frac{4(h(q)+1)^2 + 4h(q)(q-2) + q^2 - 1}{(h(q)+1)}.$$

For zeroth approximation:

$$\mathcal{N}(h(q)) = -\frac{3q}{q^2 - q + 2} + \mathcal{O}(q^2).$$

Therefore the reduced equation is

$$q' = 0 + \mathcal{O}(q^2)$$

This gives us the zero constant part. Therefore, the system of equation (38)–(39) is stable as per the Central Manifold Theory.

In conclusion, the argument summarises the point's curve $(p, 1 - p)$, which illustrates the late-time dark-energy dominated universe.

* **Critical Point $(p, -2p)$:** At this point, where $w_{\text{eff}} = 0$ and $\Omega_m = 1 + p$, it represents the dominance of matter at the background level. However, this point is unstable due to the Jacobian matrix's eigenvalues being $(3, 0)$. The energy density configuration $\Omega_m = 1 + p$ and $\Omega_Q = -p$ suggests that the matter component overwhelmingly constitutes the total energy density of the universe, considering that the value of p is exceptionally small. Consequently, this indicates that the entirety of the energy density is attributed to matter, encompassing both ordinary matter (baryonic matter) and dark matter.

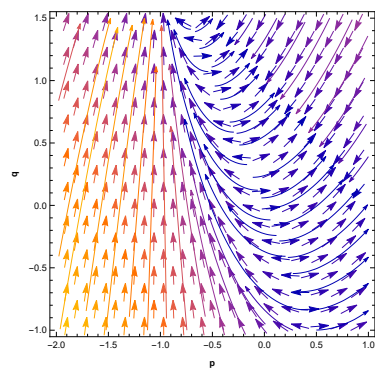


FIG. 4. Phase portrait for the dynamical system of Model II

Case 2. Matter combined with radiation

In this case the system (27)–(30) becomes

$$p' = \frac{4r + 3(1 - p - q)}{\frac{(2p+q)^2}{(p+1)} - q + 2} (q + 2p), \quad (40)$$

$$q' = \frac{4r + 3(1 - p - q)}{\frac{(2p+q)^2}{(p+1)} - q + 2} \frac{(2p + q)^2}{(p + 1)}, \quad (41)$$

$$r' = -2r \left(2 + \frac{-4r + 3(p + q - 1)}{\frac{(2p+q)^2}{(p+1)} - q + 2} \right). \quad (42)$$

In this case, the system has three curves of critical points

* **Critical Point** $(p, 1 - p, 0)$: The curve at this point, the solution depicts the dominance of dark energy component, or $\Omega_Q = 1$, where the universe undergoes acceleration characterized by $w_{\text{eff}} = -1$. This behavior closely resembles that of a cosmological constant. It becomes evident that within this scenario, the geometric aspect of the $f(Q)$ model assumes dominance over the critical point. The curve has one vanishing eigenvalue and two other eigenvalues are -4 and -3 . The stability analysis of this point is contingent upon the sign of the non-zero eigenvalues. Consequently, the curve's point maintains a consistent stability owing to this. Additionally, the critical point $(p, 1 - p, 0)$ is non-hyperbolic. The system of equations achieves asymptotic stability through the application of center manifold theory techniques.

In this case, r is the central variable, while p, q are the stable variables. The corresponding matrices are $A = \begin{pmatrix} -4 & 0 \\ 0 & -3 \end{pmatrix}$ and $B = 0$. The center manifold has now the form $p = h_1(r)$ and $q = h_2(r)$. The two components of the approximation \mathcal{N} are:

$$\begin{aligned} \mathcal{N}_1(h_1(r)) &= \\ h_1'(r) &\left(-2r \left(2 + \frac{-4r + 3(h_1(r) + h_2(r) - 1)}{\frac{(2h_1(r) + h_2(r))^2}{(h_1(r) + 1)} - h_2(r) + 2} \right) \right) - \\ &\frac{4r + 3(1 - h_1(r) - h_2(r))}{\frac{(2h_1(r) + h_2(r))^2}{(h_1(r) + 1)} - h_2(r) + 2} (h_2(r) + 2h_1(r)), \\ \mathcal{N}_2(h_2(r)) &= \\ h_2'(r) &\left(-2r \left(2 + \frac{-4r + 3(h_1(r) + h_2(r) - 1)}{\frac{(2h_1(r) + h_2(r))^2}{(h_1(r) + 1)} - h_2(r) + 2} \right) \right) - \\ &\left(\frac{4r + 3(1 - h_1(r) - h_2(r))}{\frac{(2h_1(r) + h_2(r))^2}{(h_1(r) + 1)} - h_2(r) + 2} \right) \left(\frac{(2h_1(r) + h_2(r))^2}{(h_1(r) + 1)} \right) \end{aligned}$$

For zeroth approximation:

$$\mathcal{N}_1(h_1(r)) = 0 + \mathcal{O}(r^2)$$

and

$$\mathcal{N}_2(h_2(r)) = 0 + \mathcal{O}(r^2).$$

Therefore the reduced equation is

$$r' = -r + \mathcal{O}(r^2)$$

The above equation has the negative linear part. According to the central manifold theory, the set of equations (40)–(42) is thus asymptotically stable at the equilibrium.

In conclusion, the discussion describes , the late-time dark-energy dominated universe.

* **Critical Point** $(p, -2p, 0)$: The curve of this critical point $(p, -2p, 0)$, corresponds to a solution with $\Omega_m = 1 + p$, $\Omega_Q = -p$ and $w_{\text{eff}} = 0$. Note that the value of p is very small, i.e. close to zero. This is the era where the matter component completely dominates the total energy density of the universe. However, it is saddle with eigenvalues $(3, -1, 0)$.

* **Critical Point** $(p, -2p, \frac{(1+p)}{4})$: This position, where $\Omega_m = \frac{3}{4}(1 + p)$, $\Omega_Q = -p$, $\Omega_r = \frac{(1+p)}{4}$ and $w_{\text{eff}} = \frac{1}{12}$. Since p is very small, this critical curve depicts the era where there is matter, radiations as well as dark energy . The Jacobian matrix's eigenvalues are $(4, 1, 0)$, making this point unstable.

C. MODEL III : $f(Q) = \beta + \kappa \log Q$

$$f(Q) = \beta + \kappa \log Q - Q \quad (43)$$

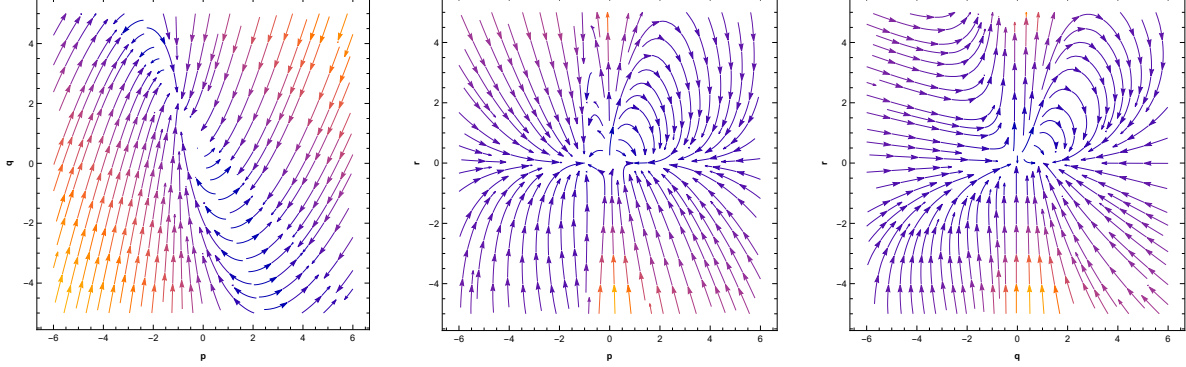
the logarithmic model, has two parameters, β and κ . This model also fits in the BBN requirements [73, 76–79] and can explain the acceleration in the late universe. As,

$$QF_{QQ} = \frac{(q-2)}{2}$$

Simple exponential functions are mathematically tractable. They can examine $f(Q)$ gravity fundamentals and provide easy analytical solutions. The mainstream cosmological model attributes the accelerated expansion of the universe to dark energy, but $f(Q)$ gravity models, even logarithmic ones, can explain it. Model predictions can be compared to cosmic gravitational interaction observations and experiments. Deviations from GR in favour of logarithmic $f(Q)$ gravity may reveal gravity's nature. They may also affect universe evolution. These factors affect cosmic structure development, cosmic microwave background radiation, and large-scale structure growth. Specific predictions can be evaluated with astrophysical and cosmic observations using logarithmic models. Logarithmic $f(Q)$ gravity can be tested against these observations to distinguish it from GR. These ideas change galactic and cosmic gravitational interactions to explain galactic rotation curves without dark matter particles. Inflationary cosmology and logarithmic models in

TABLE IV. Critical points, stability conditions, radiation and the EoS parameter.

Critical Points	Eigen-Values	Ω_m	Ω_Q	$\Omega_r = r$	w_{eff}	Stability Condition
$(p, 1-p, 0)$	$(-4, -3, 0)$	0	1	0	-1	Stable
$(p, -2p, 0)$	$(3, -1, 0)$	$1+p$	$-p$	0	0	Saddle
$(p, -2p, \frac{(1+p)}{4})$	$(4, 1, 0)$	$\frac{3}{4}(1+p)$	$-p$	$\frac{(1+p)}{4}$	$\frac{1}{12}$	Unstable

FIG. 5. Phase portrait for the dynamical system of Model II, (i)left panel($r = 0$); (ii)middle panel($q = 0$); (iii)right panel($p = 0$).

$f(Q)$ gravity affect the early universe. They can affect early universe dynamics and leave imprints on the cosmic microwave background, allowing Big Bang tests of these ideas.

In conclusion, logarithmic models in $f(Q)$ gravity can be used to evaluate alternative gravity theories and solve various astrophysical and cosmology mysteries. They allow researchers to study dark energy, General Relativity, and gravity from galaxies to the universe.

Case 1. Only matter

In this case, the system (22)–(24) becomes.

$$p' = \frac{3(1-p-q)}{q-2}(q+2p), \quad (44)$$

$$q' = \frac{3(1-p-q)}{q-2}2(q-2), \quad (45)$$

There is only one corresponding critical point.

* **Critical Point** $(p, 1-p)$: The curve at this point is consistent with the energy density $\Omega_m = 0$ solution, proving that matter has no effect on the universe's overall energy density. According to the energy density $\Omega_Q = 1$, dark energy dominates the overall energy density of the universe. This would imply that the universe accelerates with $w_{\text{eff}} = -1$, which is compatible with the behaviour of a cosmological constant, and that the apparent rapid expansion is solely due to the repulsive effects of dark energy, with no contribution from matter.

The critical point $(p, 1-p)$ is non-hyperbolic and -3 is the other eigenvalue. Looking at the non-vanishing eigenvalue, the curve is stable. Also, we found that the

system of equations is asymptotically stable using the center manifold theory.

In this case p and q are the stable and center variables respectively. The corresponding matrices are $A = -3$ and $B = 0$. The center manifold has now the form $p = h(q)$; the approximation \mathcal{N} is given by

$$\mathcal{N}(h(q)) = h'(q) \frac{3(1-h(q)-q)}{u(q)-q+2} u(q) - \frac{3(1-h(q)-q)}{u(q)-q+2} (q+2h(q))$$

$$\text{where } u(q) = \frac{4(h(q)+1)^2 + 4h(q)(q-2) + q^2 - 1}{(h(q)+1)}$$

For zeroth approximation:

$$\mathcal{N}(h(q)) = -\frac{3q}{q-2} + \mathcal{O}(q^2)$$

Therefore the reduced equation is

$$q' = -18 + \mathcal{O}(q^2)$$

This provides us with the negative constant portion. According to the central manifold theory, the system of equations (44)–(45) is asymptotically stable at the equilibrium point.

The argument summarises the point's curve $(p, 1-p)$, which is the late universe's dark-energy-dominated universe.

Case 2. Matter combined with radiation

In this case, the system (27)–(30) becomes.

$$p' = \frac{4r - 3(p+q-1)}{q-2}(q+2p), \quad (46)$$

$$q' = \frac{4r - 3(p+q-1)}{q-2}2(q-2), \quad (47)$$

TABLE V. Critical Points, Stability Conditions and EoS parameter.

Critical Points	Eigen-Values	Ω_m	Ω_Q	w_{eff}	Stability Condition
$(p, 1-p)$	$(-3, 0)$	0	1	-1	Stable

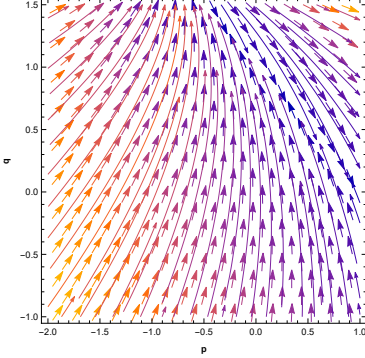


FIG. 6. Phase portrait for the dynamical system of Model III.

$$r' = -2r \left(2 + \frac{-4r + 3(p + q - 1)}{q - 2} \right). \quad (48)$$

The above dynamical system has one critical point.

* **Critical Point** $(p, 1-p, 0)$: The curve at this point is consistent with the energy density $\Omega_m = 0$ solution, proving that matter has no effect on the universe's overall energy density. According to the energy density $\Omega_Q = 1$, dark energy dominates the overall energy density of the universe. This would imply that the universe accelerates with $w_{\text{eff}} = -1$, which is compatible with the behaviour of a cosmological constant, and that the apparent rapid expansion is solely due to the repulsive effects of dark energy, with no contribution from matter. The curve has one vanishing eigenvalue and two additional eigenvalues, -4 and -3 . It is one-dimensional. Examining the non-zero eigenvalue signature allows one to determine whether the curve is stable. As a result, the curve at the point is constantly stable. Furthermore, since the related Jacobian matrix has just one vanishing eigenvalue, the critical point $(p, 1-p, 0)$ is non-hyperbolic. We find that the system of equations is asymptotically stable by applying the center manifold theory method.

The central variable in this instance is r , and the stable variables are p, q . The corresponding matrices are $A = \begin{pmatrix} -4 & 0 \\ 0 & -3 \end{pmatrix}$ and $B = 0$. Now, the center manifold has the form $p = h_1(r)$ and $q = h_2(r)$; the approximation \mathcal{N} has two components:

$$\begin{aligned} \mathcal{N}_1(h_1(r)) = & \\ h_1'(r) \left(-2r \left(2 + \frac{-4r + 3(h_1(r) + h_2(r) - 1)}{(2h_1(r) + h_2(r))^2 - h_2(r) + 2} \right) \right) - & \\ \left(\frac{4r + 3(1 - h_1(r) - h_2(r))}{(2h_1(r) + h_2(r))^2 - h_2(r) + 2} \right) (h_2(r) + 2h_1(r)), & \end{aligned}$$

$$\begin{aligned} \mathcal{N}_2(h_2(r)) = & \\ h_2'(r) \left(-2r \left(2 + \frac{-4r + 3(h_1(r) + h_2(r) - 1)}{(2h_1(r) + h_2(r))^2 - h_2(r) + 2} \right) \right) - & \\ \left(\frac{4r + 3(1 - h_1(r) - h_2(r))}{(2h_1(r) + h_2(r))^2 - h_2(r) + 2} \right) \left(\frac{(2h_1(r) + h_2(r))^2}{(h_1(r) + 1)} \right) & \end{aligned}$$

For zeroth approximation:

$$\mathcal{N}_1(h_1(r)) = 0 + \mathcal{O}(r^2)$$

and

$$\mathcal{N}_2(h_2(r)) = -8r - 6 + \mathcal{O}(r^2).$$

Therefore the reduced equation gives us

$$r' = -6r + \mathcal{O}(r^2)$$

This provides us with the negative constant portion. According to the central manifold theory, the system of equations (46)-(48) is asymptotically stable at the equilibrium point.

The argument summarises the point's curve $(p, 1-p, 0)$, which is the late time dark-energy-dominated universe.

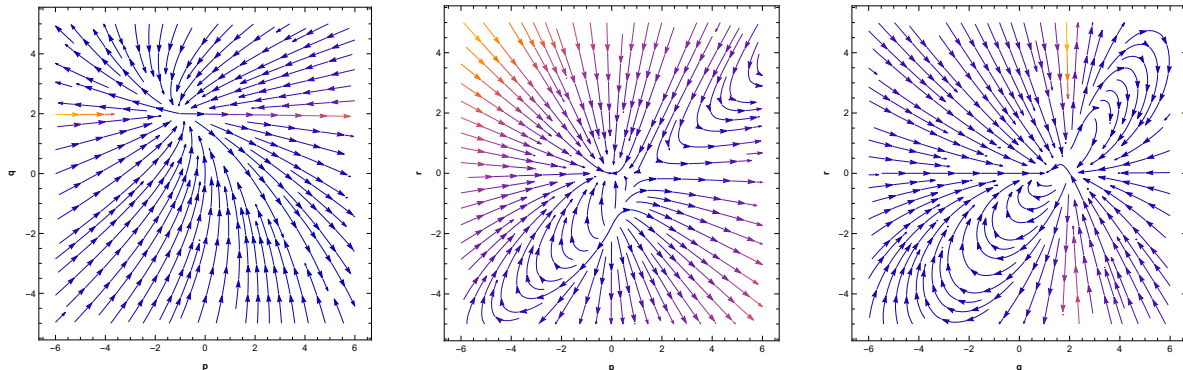
In Fig. 8, it can be seen that the universe is initially completely filled with radiation, which subsequently gradually decreases and matter begins to form, increasing the relative energy density. So w_{eff} behaves similarly to the energy density of radiation until dark energy enters the picture. Later on, dark energy takes over and causes the accelerated expansion of the universe that we are currently observing. The parameter w_{eff} starts at -0.55 when the universe was totally dominated by radiation, then drops during the matter formation era, then gets negative when dark energy begins to dominate, and finally reaches the value of w_{eff} , which is -1 .

V. CONCLUSIONS AND DISCUSSIONS

In the current study, we coupled the dynamical system analysis of the background equations to test the validity of the findings using an independent approach. The flat FLRW metric is regarded to be the best description of the universe. This research was inspired by the fact that $f(Q)$ gravity-based cosmological models are particularly effective at fitting observable datasets at both background levels. Following the conversion of the background equations into an autonomous framework, our investigation on prevalent models found in literature, concentrating on the power-law, exponential, and logarithmic higher-curvature gravity models augmented by a boundary terms. In the work, we have considered two

TABLE VI. Critical points, stability conditions and the EoS parameter.

Critical Points	Eigen-Values	Ω_m	Ω_Q	$\Omega_r = r$	w_{eff}	Stability Condition
$(p, 1-p, 0)$	$(-4, -3, 0)$	0	1	0	-1	Stable

FIG. 7. Phase portrait for the dynamical system of Model III, (i)left panel($r = 0$); (ii)middle panel($q = 0$); (iii)right panel($p = 0$).

cases: “Case I- only matter” and “Case II- Matter combined with radiation without interaction” for each model.

In the power-law model represented by $f(Q) = Q + \kappa(\frac{Q}{Q_0})^n$, the scenario involving only matter revealed two critical points. Among these, the equilibrium point at $(p, 1-p)$ emerged as asymptotically stable through the application of center manifold theory. This critical point’s significance lies in asserting the dominance of dark energy during the later phases of the universe. It signifies that the universe’s accelerated expansion solely stems from the repulsive effects of dark energy, without any contribution from matter. On the other hand, the point $(0, 0)$ behaved as a saddle point for $n > 1$ and proved to be unstable for $n \leq 1$. This specific point denotes the epoch where matter formation reaches completion. Our depiction of phase portraits in Fig. 1 provides a visual representation, enhancing the comprehension of these behaviors at these critical points.

In the scenario involving matter combined with radiation without any interaction, our analysis unveiled three critical points, among which the point $(p, 1-p, 0)$ emerged as asymptotically stable, employing center manifold theory. This specific point on the curve signifies a solution where the dominance of an effective dark energy component leads to the universe accelerating with $w_{\text{eff}} = -1$, aligning with the behavior akin to a cosmological constant. Contrarily, the point $(0, 0, 0)$ exhibited saddle-like behavior with eigenvalues $(3, -1, -3(n-1))$ across all n values. Our observations indicate trajectories converging towards a stable late-time point, passing through it, and subsequently diverging from it. We hypothesize that this particular point might serve as the most plausible candidate for elucidating the development of structures during the matter-dominated epoch at background levels. The point $(0, 0, \frac{1}{4})$ was found to be saddle for $n > 1$ and unstable for $n \leq 1$. This critical point

depicts the period where matter, radiation, and dark energy are present together. Additionally, we plotted phase portraits in Fig. 2, which provides a clearer representation of the behavior at those points. Fig. 3 illustrates how the energy density parameter can be used to display the behavior of dark energy versus $\ln a$ in order to comprehend its dominance in various ages of the cosmos.

In the exponential model $f(Q) = Qe^{\kappa(\frac{Q}{Q_0})}$, for matter case, two critical points were obtained, out of which the point $(p, 1-p)$ was found to be asymptotically stable by using center manifold theory with the eigen-values $(-3, 0)$ and the point $(p, -2p)$ was unstable. The critical point $(p, 1-p)$ indicates that dark energy predominates in the late universe and that matter has no impact on its repulsive effects, which are responsible for the universe’s observable accelerated expansion. This critical point depicts the era of the late-time-dark-energy dominated universe. The critical point $(p, -2p)$ depicts the era where the matter component completely dominates the total energy density of the universe.

For matter combined with radiation case i.e case II, there were three critical points, out of which $(p, 1-p, 0)$ point with the eigen-value $(-4, -3, 0)$ was found to be asymptotically stable at equilibrium points by using center manifold theory. The curve at this point depicts a solution where the universe accelerates with $w_{\text{eff}} = -1$ and the effective dark energy component predominates, which is in line with the behavior of a cosmological constant. The points $(p, -2p, 0)$ and $(p, -2p, \frac{(1+p)}{4})$ were saddle and unstable respectively. In phase portrait, Figs. 4 and 5, the behavior at those points is well depicted.

In the logarithmic model characterized by $f(Q) = \beta + \kappa \log Q$, we encountered a single critical point for both scenarios: the matter-only case yielded $(p, 1-p)$, while the matter combined with radiation scenario resulted in $(p, 1-p, 0)$. Utilizing center manifold theory, our anal-

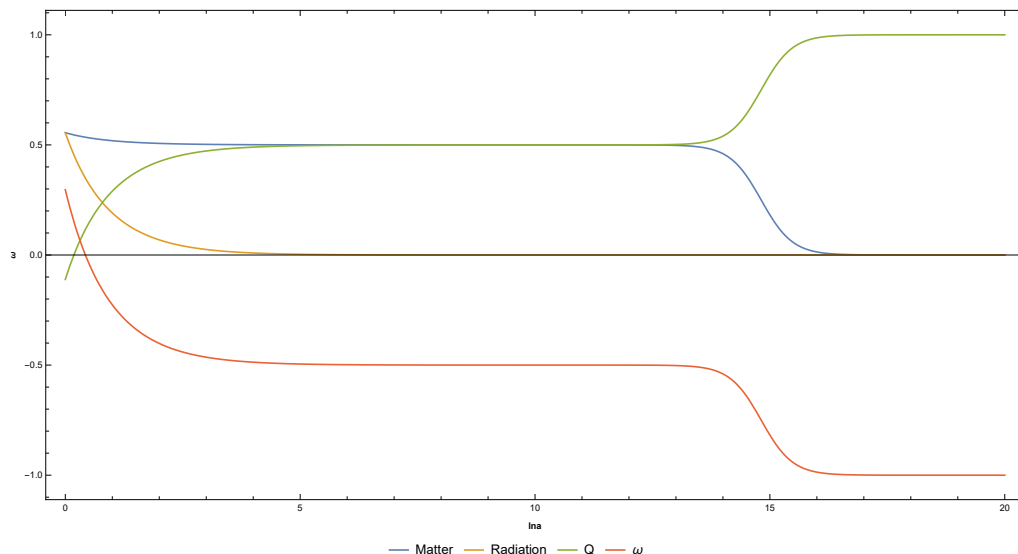


FIG. 8. Evolution of matter, radiation, Dark energy and the EoS parameter in the logarithmic model.

ysis indicated that in both cases, these points proved to be asymptotically stable at their respective equilibrium states. Moreover, these critical points corresponded to curves indicative of matter dominance. In Figs. 6 and 7, we illustrated phase portraits to offer a more detailed insight into the behaviors exhibited at these critical points. To further elucidate the dominance of dark energy across different cosmic eras, we delved into the energy density parameter. In Fig. 8, we demonstrated the behavior of this parameter plotted against $\ln a$, providing a comprehensive understanding of dark energy's prevalence throughout various epochs of the universe.

As a concluding note, this study successfully demonstrates stability and acceleration phases within the universe's evolution without the inclusion of an "unobserved" entity like dark energy. The models explored in this article portray these phenomena without necessitating the introduction of such an additional component, offering valuable insights into cosmic dynamics while relying

solely on observable quantities.

This research could be extended by taking into account more $f(Q)$ gravity models that meet the BBN (Big-Bang Nucleosynthesis) constraints and all viability requirements. In addition to this, other categories of modification such as $f(Q, T)$ or Weyl-type theories might be taken into account, and further applications of dynamical system analysis could be made as well as stability analyses for such cases could be carried out. Several forms of linear and nonlinear interactions could also be studied with modification in the gravity.

ACKNOWLEDGEMENT

The work of KB was partially supported by the JSPS KAKENHI Grant Number 21K03547 and 23KF0008.

-
- [1] S. Perlmutter *et al.* [Supernova Cosmology Project], *Astrophys. J.* **517**, 565-586 (1999).
 - [2] A. G. Riess *et al.* [Supernova Search Team], *Astron. J.* **116**, 1009-1038 (1998).
 - [3] A. G. Riess *et al.* [Supernova Search Team], *Astrophys. J.* **607**, 665-687 (2004).
 - [4] N. Aghanim *et al.* [Planck], *Astron. Astrophys.* **641**, A6 (2020) [erratum: *Astron. Astrophys.* **652**, C4 (2021)].
 - [5] T. Koivisto and D. F. Mota, *Phys. Rev. D* **73**, 083502 (2006).
 - [6] S. F. Daniel, R. R. Caldwell, A. Cooray and A. Melchiorri, *Phys. Rev. D* **77**, 103513 (2008).
 - [7] D. J. Eisenstein *et al.* [SDSS], *Astrophys. J.* **633**, 560-574 (2005).
 - [8] E. J. Copeland, M. Sami and S. Tsujikawa, *Int. J. Mod. Phys. D* **15**, 1753-1936 (2006).
 - [9] T. Padmanabhan, *Gen. Rel. Grav.* **40**, 529-564 (2008).
 - [10] R. Durrer and R. Maartens, *Gen. Rel. Grav.* **40**, 301-328 (2008).
 - [11] K. Bamba, S. Capozziello, S. Nojiri and S. D. Odintsov, *Astrophys. Space Sci.* **342**, 155-228 (2012).
 - [12] R. Kase and S. Tsujikawa, *Int. J. Mod. Phys. D* **28**, no.05, 1942005 (2019).
 - [13] N. Aghanim *et al.* [Planck], *Astron. Astrophys.* **641**, A6 (2020) [erratum: *Astron. Astrophys.* **652**, C4 (2021)].
 - [14] B. Ratra and P. J. E. Peebles, *Phys. Rev. D* **37**, 3406 (1988).
 - [15] R. R. Caldwell, R. Dave and P. J. Steinhardt, *Phys. Rev. Lett.* **80**, 1582-1585 (1998).

- [16] R. R. Caldwell, Phys. Lett. B **545**, 23-29 (2002).
- [17] B. Feng, X. L. Wang and X. M. Zhang, Phys. Lett. B **607**, 35-41 (2005).
- [18] R. Bean, D. J. H. Chung and G. Geshnizjani, Phys. Rev. D **78**, 023517 (2008).
- [19] D. Langlois, Int. J. Mod. Phys. D **28**, no.05, 1942006 (2019).
- [20] T. Koivisto, Int. J. Geom. Meth. Mod. Phys. **15**, 1840006 (2018).
- [21] H. A. Buchdahl, Mon. Not. Roy. Astron. Soc. **150**, 1 (1970).
- [22] T. P. Sotiriou and V. Faraoni, Rev. Mod. Phys. **82**, 451-497 (2010).
- [23] A. A. Starobinsky, Phys. Lett. B **91**, 99-102 (1980).
- [24] D. J. Brooker, S. D. Odintsov and R. P. Woodard, Nucl. Phys. B **911**, 318-337 (2016).
- [25] Q. G. Huang, JCAP **02**, 035 (2014).
- [26] S. Nojiri, S. D. Odintsov and V. K. Oikonomou, Phys. Rept. **692**, 1-104 (2017).
- [27] S. Capozziello and M. De Laurentis, Phys. Rept. **509**, 167-321 (2011).
- [28] A. De Felice and S. Tsujikawa, Living Rev. Rel. **13**, 3 (2010).
- [29] S. Nojiri and S. D. Odintsov, Phys. Rept. **505**, 59-144 (2011).
- [30] S. Arai, K. Aoki, Y. Chinone, R. Kimura, T. Kobayashi, H. Miyatake, D. Yamauchi, S. Yokoyama, K. Akitsu and T. Hiramatsu, *et al.* PTEP **2023**, no.7, 072E01 (2023).
- [31] T. Harko, F. S. N. Lobo, S. Nojiri and S. D. Odintsov, Phys. Rev. D **84**, 024020 (2011).
- [32] S. Capozziello and M. De Laurentis, Phys. Rept. **509**, (2011) 167-321.
- [33] T. Clifton, P. G. Ferreira, A. Padilla and C. Skordis, Phys. Rept. **513**, 1-189 (2012).
- [34] S. Capozziello, V. De Falco and C. Ferrara, Eur. Phys. J. C **83**, no.10, 915 (2023)
- [35] A. Joyce, B. Jain, J. Khoury and M. Trodden, Phys. Rept. **568**, 1-98 (2015).
- [36] M. Koussour, S. H. Shekh, A. Hanin, Z. Sakhi, S. R. Bhojer and M. Bennai, Class. Quant. Grav. **39**, no.19, 195021 (2022).
- [37] R. Ferraro and F. Fiorini, Phys. Rev. D **75**, 084031 (2007).
- [38] Y. F. Cai, S. Capozziello, M. De Laurentis and E. N. Saridakis, Rept. Prog. Phys. **79**, no.10, 106901 (2016).
- [39] S. Bahamonde, K. F. Dialektopoulos, C. Escamilla-Rivera, G. Farrugia, V. Gakis, M. Hendry, M. Hohmann, J. Levi Said, J. Mifsud and E. Di Valentino, Rept. Prog. Phys. **86**, no.2, 026901 (2023).
- [40] J. Beltrán Jiménez, L. Heisenberg and T. Koivisto, Phys. Rev. D **98**, no.4, 044048 (2018).
- [41] J. Beltrán Jiménez, L. Heisenberg, T. S. Koivisto and S. Pekar, Phys. Rev. D **101**, no.10, 103507 (2020).
- [42] L. Heisenberg, [arXiv:2309.15958 [gr-qc]].
- [43] S. Mandal, P. K. Sahoo and J. R. L. Santos, Phys. Rev. D **102**, no.2, 024057 (2020).
- [44] S. Mandal, D. Wang and P. K. Sahoo, Phys. Rev. D **102**, 124029 (2020).
- [45] T. Harko, T. S. Koivisto, F. S. N. Lobo, G. J. Olmo and D. Rubiera-Garcia, Phys. Rev. D **98**, no.8, 084043 (2018).
- [46] N. Dimakis, A. Paliathanasis and T. Christodoulakis, Class. Quant. Grav. **38**, no.22, 225003 (2021).
- [47] M. Koussour, S. H. Shekh and M. Bennai, JHEAp **35**, 43-51 (2022).
- [48] M. Koussour, S. H. Shekh and M. Bennai, Phys. Dark Univ. **36**, 101051 (2022).
- [49] S. A. Narawade, S. P. Singh and B. Mishra, Phys. Dark Univ. **42**, 101282 (2023)
- [50] A. S. Agrawal, B. Mishra and S. K. Tripathy, JHEAp **38**, 41-48 (2023)
- [51] L. Pati, S. A. Kadam, S. K. Tripathy and B. Mishra, Phys. Dark Univ. **35**, 100925 (2022)
- [52] S. D. Odintsov and V. K. Oikonomou, Phys. Rev. D **96**, no.10, 104049 (2017).
- [53] S. D. Odintsov, V. K. Oikonomou and P. V. Tretyakov, Phys. Rev. D **96**, no.4, 044022 (2017).
- [54] M. Hohmann, L. Jarv and U. Ualikhanova, Phys. Rev. D **96**, no.4, 043508 (2017).
- [55] S. D. Odintsov and V. K. Oikonomou, Phys. Rev. D **98**, no.2, 024013 (2018).
- [56] S. D. Odintsov and V. K. Oikonomou, Class. Quant. Grav. **36**, no.6, 065008 (2019).
- [57] S. Santos Da Costa, F. V. Roig, J. S. Alcaniz, S. Capozziello, M. De Laurentis and M. Benetti, Class. Quant. Grav. **35**, no.7, 075013 (2018).
- [58] P. Shah, G. C. Samanta and S. Capozziello, Int. J. Mod. Phys. A **33**, no.18n19, 1850116 (2018).
- [59] M. K. Sharma and S. Sur, Phys. Dark Univ. **40**, 101192 (2023) doi:10.1016/j.dark.2023.101192 [arXiv:2112.14017 [astro-ph.CO]].
- [60] P. Shah and G. C. Samanta, Eur. Phys. J. C **79**, no.5, 414 (2019).
- [61] Ellis, George Francis Rayner, and John Wainwright, eds. Dynamical systems in cosmology. Cambridge University Press, 1997.
- [62] A. A. Coley, "Dynamical systems and cosmology," Kluwer, (2003).
- [63] P. Vishwakarma and P. Shah, Int. J. Mod. Phys. D **32**, no.11, 2350071 (2023)
- [64] J. de Haro, S. Nojiri, S. D. Odintsov, V. K. Oikonomou and S. Pan, Phys. Rept. **1034**, 1-114 (2023).
- [65] M. Nakahara, "Geometry, topology and physics", (2003).
- [66] W. Khylllep, J. Dutta, S. Basilakos and E. N. Saridakis, Phys. Rev. D **105**, no.4, 043511 (2022).
- [67] J. Beltrán Jiménez and T. S. Koivisto, Universe **7**, no.5, 143 (2021)
- [68] D. A. Gomes, J. Beltrán Jiménez, A. J. Cano and T. S. Koivisto, [arXiv:2311.04201 [gr-qc]].
- [69] W. Khylllep, J. Dutta, E. N. Saridakis and K. Yesmakhanova, Phys. Rev. D **107**, no.4, 044022 (2023).
- [70] P. Shah and G. C. Samanta, Int. J. Mod. Phys. A **35**, no.22, 2050124 (2020).
- [71] J. Beltrán Jiménez, L. Heisenberg and T. S. Koivisto, JCAP **08**, 039 (2018).
- [72] G. N. Gadbail, S. Arora and P. K. Sahoo, Phys. Lett. B **838**, 137710 (2023).
- [73] F. K. Agnastopoulos, V. Gakis, E. N. Saridakis and S. Basilakos, Eur. Phys. J. C **83**, no.1, 58 (2023).
- [74] S. Bahamonde, C. G. Böhmmer, S. Carloni, E. J. Copeland, W. Fang and N. Tamanini, Phys. Rept. **775-777**, 1-122 (2018).
- [75] N. Tamanini, "Dynamical systems in dark energy models," (2014).
- [76] R. H. Cyburt, B. D. Fields, K. A. Olive and T. H. Yeh, Rev. Mod. Phys. **88**, 015004 (2016).

- [77] J. D. Barrow, S. Basilakos and E. N. Saridakis, Phys. Lett. B **815**, 136134 (2021).
- [78] P. Asimakis, S. Basilakos, N. E. Mavromatos and E. N. Saridakis, Phys. Rev. D **105**, no.8, 084010 (2022).
- [79] P. Vishwakarma and P. Shah, Eur. Phys. J. C **84**, no.2, 159 (2024).
- [80] F. K. Anagnostopoulos, S. Basilakos and E. N. Saridakis, Phys. Lett. B **822**, 136634 (2021).